

Dipper disks not inclined towards edge-on orbits

M. Ansdell,¹ E. Gaidos,^{2,3} J. P. Williams,¹ G. Kennedy,⁴ M. C. Wyatt,⁴
D. M. LaCourse,⁵ T. L. Jacobs,⁵ A. W. Mann⁶

¹*Institute for Astronomy, University of Hawai‘i at Mānoa, Honolulu, HI, USA*

²*Department of Geology & Geophysics, University of Hawai‘i at Mānoa, Honolulu, HI, USA*

³*Center for Space and Habitability, University of Bern, Bern, Switzerland*

⁴*Institute of Astronomy, University of Cambridge, Madingley Road, Cambridge, UK*

⁵*Amateur Astronomer*

⁶*Hubble Fellow, Department of Astronomy, The University of Texas at Austin, Austin, TX, USA*

Accepted to MNRAS Letters

ABSTRACT

The so-called “dipper” stars host circumstellar disks and have optical and infrared light curves that exhibit quasi-periodic or aperiodic dimming events consistent with extinction by transiting dusty structures orbiting in the inner disk. Most of the proposed mechanisms explaining the dips—i.e., occulting disk warps, vortices, and forming planetesimals—assume nearly edge-on viewing geometries. However, our analysis of the three known dippers with publicly available resolved sub-mm data reveals disks with a range of inclinations, most notably the face-on transition disk J1604-2130 (EPIC 204638512). This suggests that nearly edge-on viewing geometries are *not* a defining characteristic of the dippers and that additional models should be explored. If confirmed by further observations of more dippers, this would point to inner disk processes that regularly produce dusty structures far above the outer disk midplane in regions relevant to planet formation.

Key words: protoplanetary discs – stars: variables: T Tauri – planet-disc interactions

1 INTRODUCTION

Understanding how planets form is one of the most compelling problems in astronomy. Close-in planets appear to be common (Howard et al. 2010; Petigura et al. 2013; Silburt et al. 2015) and we can study their nascent systems (i.e., protoplanetary disks) in young stellar associations. However, observing planet formation at $\lesssim 1$ AU is complicated by small angular scales and faint disk emission compared to the host star; for the nearest star-forming regions, the best achievable angular resolution for optical/infrared scattered light and sub-mm images is only a few AU.

However, new probes of the inner disk may be the so-called “dipper” stars, whose optical and infrared light curves exhibit episodic drops in flux consistent with extinction by transiting dusty structures orbiting with Keplerian periods of down to a few days. Dipper stars were identified with the CoRoT and *Spitzer* missions in the young (~ 2 – 3 Myr) Orion Nebula Cluster (Morales-Calderón et al. 2011) and NGC 2264 region (Alencar et al. 2010; Cody et al. 2014). These studies found that the depth, duration, and periodicity of the dips are consistent with extinction by dust orbiting near the star-disk co-rotation radius. McGinnis et al. (2015) proposed that the dippers in NGC 2264 could be explained by occulting inner disk warps driven by accretion streams

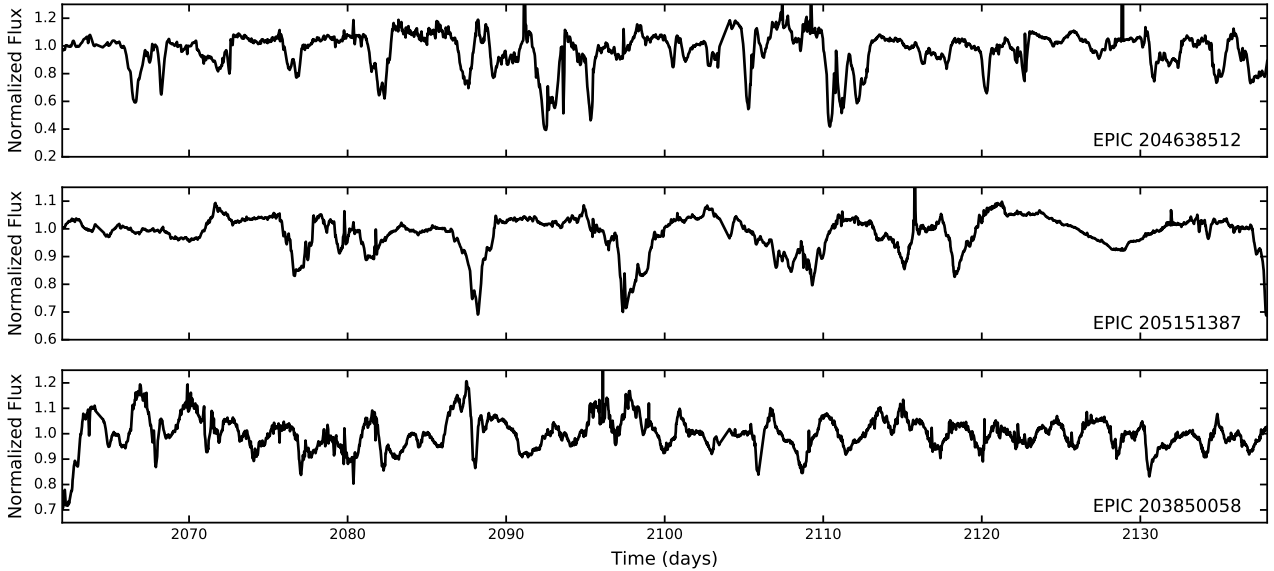
onto the host star, as reported for AA Tau (Bouvier et al. 1999). Unfortunately, the significant distances to these clusters (~ 400 – 750 pc) limited follow-up observations.

Ansdell et al. (2016) identified ~ 25 dippers in the young ($\lesssim 10$ Myr), nearby (~ 120 – 145 Myr) Upper Sco and ρ Oph star-forming regions using high-precision optical photometry from the K2 mission (Howell et al. 2014). Follow-up observations showed that the K2 dippers are often weakly accreting late-type stars hosting moderately evolved primordial disks, challenging the disk warp scenario described above. Thus Ansdell et al. (2016) proposed alternative mechanisms to explain the dips, namely occulting vortices at the inner disk edge produced by the Rossby Wave Instability and transiting clumps of circumstellar material related to planetesimal formation. Bodman et al. (2016) also found that magnetospheric truncation of weakly accreting disks with misaligned magnetic fields could form occulting accretion streams that produce dippers with high to moderate inclinations.

The proposed mechanisms for explaining the dips therefore assume geometries that are closer to edge-on than face-on. The occurrence rate of dippers in co-eval clusters (e.g., ~ 20 – 30% of classical T Tauri stars in NGC 2264; Alencar et al. 2010, Cody et al. 2014) and the moderate optical extinction towards these objects ($A_V \lesssim 1$; Ansdell et al. 2016) suggest that we are not seeing the disks directly edge-on

Table 1. Properties of Dippers with Resolved Sub-mm Images

EPIC	2MASS	RA _{J2000}	Dec _{J2000}	Mem.	SpT	T_{eff} (K)	A_V (mag)	Disk	P_{rot} (d)	D_{dip}	Var.
204638512	16042165-2130284	16:04:21.655	-21:30:28.50	USc	K2	4900	0.7	TD	5.00	0.57	A
205151387	16090075-1908526	16:09:00.762	-19:08:52.70	USc	M1	4000	0.8	Full	9.55	0.31	Q
203850058	16253849-2613540	16:27:06.596	-24:41:48.84	Oph	M6	2700	3.0	Full	2.88	0.18	Q

**Figure 1.** Normalized K2 light curves (Section 3.1) showing $\gtrsim 10\%$ dip depths with ~ 0.5 – 2 day durations typical of dipper stars.

($i = 90^\circ$), but rather viewing the dippers at nearly edge-on inclinations (e.g., $i = 70^\circ$) and thus observing transits of dusty structures lifted above the disk midplane. However, these geometric assumptions have not yet been compared to observations.

In this Letter, we present the three known dippers whose circumstellar disks have been resolved in archival sub-mm data such that their inclinations can be constrained. Surprisingly, we find disks with a range of inclinations, most notably the face-on transition disk (TD) J1604-2130 (Mathews et al. 2012; Zhang et al. 2014). This indicates that nearly edge-on disk inclinations are *not* a defining characteristic of the dippers, and motivates a re-examination of the dipper mechanisms so that we can properly interpret these objects in the context of planet formation.

2 SAMPLE

Our sample consists of the three dippers with publicly available high-resolution sub-mm data sufficient to constrain disk inclinations. The dippers were identified from their K2 light curves and are located in the ~ 10 -Myr old Upper Sco (Pecaut et al. 2012) and ~ 1 -Myr old ρ Oph (Andrews & Williams 2007) star-forming regions. EPIC 205151387 and EPIC 203850058 were reported in Ansdell et al. (2016), while EPIC 204638512 is a newly identified dipper. To our knowledge, these are the only currently known dippers with resolved sub-mm data. Table 1 gives their Ecliptic Plane Input

Catalog (EPIC) and Two Micron All-Sky Survey (2MASS; Skrutskie et al. 2006) names, right ascension and declination, cluster membership (Mem.), spectral type (SpT), effective temperature (T_{eff}), optical extinction (A_V), and disk type (Disk). Stellar properties are from the literature (Natta et al. 2002; Carpenter et al. 2014; Ansdell et al. 2016).

EPIC 204638512 is a K-type pre-main sequence star with spectroscopic signatures of weak accretion (e.g., Dahm et al. 2012) and hosts the face-on TD known as J1604-2130 (Mathews et al. 2012; Zhang et al. 2014). EPIC 205151387 is a pre-main sequence M1 star that hosts a full disk (Carpenter et al. 2014) and exhibits variable accretion signatures (Dahm et al. 2012; Ansdell et al. 2016). EPIC 203850058 is the brown dwarf ρ Oph 102, which hosts a well-studied full disk (Natta et al. 2002; Ricci et al. 2012) that shows evidence for significant mass accretion as well as winds and molecular outflows (Natta et al. 2004; Whelan et al. 2005; Phan-Bao et al. 2008; McClure et al. 2010; Manara et al. 2015).

3 DATA & ANALYSIS

3.1 K2 Optical Light Curves

Figure 1 presents the K2 light curves of the three dippers in our sample. As in Ansdell et al. (2016), we use the K2SFF light curves made publicly available by the Mikulski Archive for Space Telescopes (MAST). These light curves were extracted from the *Kepler* Target Pixel Files (TPFs) using photometric apertures with the Self Field Flattening (SFF)

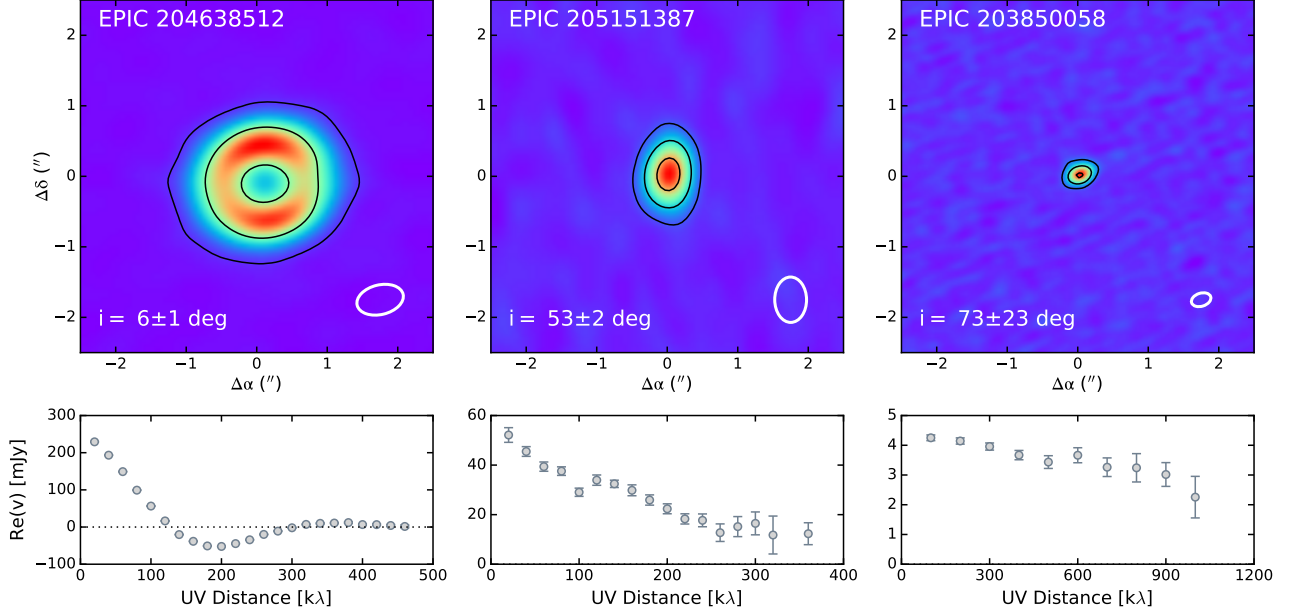


Figure 2. Top panels show ALMA sub-mm continuum images ($5'' \times 5''$) with fitted disk inclinations and beam sizes (Section 3.2 & 4.1). Contours are 10σ and 100σ for EPIC 204638512 and 5σ , 20σ , and 50σ for EPIC 205151387 and EPIC 203850058. Bottom panels show the real part of the visibilities as a function of projected baseline length.

technique, which corrects for spacecraft motion by correlating observed flux variability with spacecraft pointing (Vanderburg & Johnson 2014).

For EPIC 204638512 and EPIC 205151387, fainter secondary sources are visible within their K2SFF photometric apertures. However, these potentially contaminating interlopers are at sufficiently large projected distances ($>8''$) from the primary targets that their separate light curves can be manually extracted. We obtained the TPFs from MAST and used the KEPPCA pipeline to apply custom photometric apertures for individually extracting the light curves of the primary and secondary sources while also correcting for spacecraft motion. We confirmed that the dipper activity is associated with the primary target with negligible contributions from the secondary source in both cases. We use the K2SFF light curves in the remainder of this work, as they show improved pointing error corrections compared to the light curves produced by our KEPPCA pipeline.

We used the K2 light curves to infer stellar rotation periods (P_{rot}) and characterize the dipper activity in terms of dip depth (D_{dip}) and quasi-periodic (Q) or aperiodic (A) variability (see Section 2.2 in Ansdell et al. 2016). Table 1 provides these dipper properties, though the P_{rot} of EPIC 204638512 is uncertain due to a weak rotational signal. The three dippers in our sample generally follow the trends with stellar and disk properties identified in Ansdell et al. (2016), indicating that they are not unusual among the overall dipper population. In particular, they follow the correlation between extinction-corrected WISE-2 excess and D_{dip} (see Figure 9 in Ansdell et al. 2016), which was interpreted as evidence that the dips are related to hot inner (rather than cool outer) disk material. The three dippers also follow the observed correlation between P_{rot} and T_{eff} , although EPIC 205151387 has a long P_{rot} for its T_{eff} value. SED modeling by Ansdell et al. (2016) also showed that dip-

pers typically have inner dust disks extending to within a few stellar radii. The infrared color excesses for EPIC 205151387 and EPIC 203850058 indicate they host full disks (see Figure 6 in Ansdell et al. 2016). Although EPIC 204638512 hosts a disk with a large inner cavity in the sub-mm, it exhibits variable infrared excess consistent with dust at small ($\lesssim 0.1$ AU) orbital radii (Dahm 2010; Zhang et al. 2014).

3.2 Resolved Sub-mm Data

EPIC 204638512 hosts the well-characterized face-on TD known as J1604-2130, which was discovered by Mathews et al. (2012) using the Sub-millimeter Array (SMA; Ho et al. 2004). Mathews et al. (2012) resolved a ~ 70 -AU inner dust cavity in their continuum map and derived a precise disk inclination of $6^\circ \pm 1.5^\circ$ using their ^{12}CO 3–2 first-moment map. Zhang et al. (2014) later compared the dust and gas radial structures using ALMA Cycle 0 observations; Figure 2 shows the cleaned $880 \mu\text{m}$ continuum image from the ALMA Science Archive (project code: 2011.0.00526.S) with a clearly resolved source and $0.67'' \times 0.42''$ ($\sim 100 \times 60$ AU) beam.

EPIC 205151387 was also observed during ALMA Cycle 0 (project code: 2011.0.00526.S) in the $880 \mu\text{m}$ continuum and ^{12}CO 3–2 line (Carpenter et al. 2014). Figure 2 shows the cleaned continuum image from the ALMA Science Archive with a $0.64'' \times 0.45''$ ($\sim 95 \times 65$ AU) beam. We also plot the real part of the visibilities as a function of projected baseline length, where the clear decrease in visibility with UV distance indicates a spatially resolved source.

EPIC 203850058 was imaged at high resolution in the $870 \mu\text{m}$ continuum during ALMA Cycle 1 (project code: 2012.1.00046.S). The calibrated continuum data were not available from the ALMA Science Archive, thus we downloaded the raw visibilities and executed the pipeline calibration script, then extracted the continuum image by averaging

ing over the continuum channels and interactively cleaning with a Briggs robust weighting parameter of +0.5, giving a beam size of $0.28'' \times 0.19''$ ($\sim 35 \times 25$ AU). Figure 2 shows the cleaned continuum image and the real part of the visibilities as a function of projected baseline length; the slight decrease in the visibilities indicates a marginally resolved source.

3.3 Adaptive Optics Imaging

We searched the literature for adaptive optics (AO) imagery to check whether close companions could be influencing the dips. EPIC 204638512 has been imaged extensively with AO, providing strict limits on close companions. Kraus et al. (2008) used aperture masking interferometry combined with direct imaging to rule out the presence of close companions from $\sim 0.07 M_{\odot}$ at ~ 2 AU to $\sim 0.02 M_{\odot}$ at ~ 40 AU. Ireland et al. (2011) used direct imaging to limit companions from $\sim 0.07 M_{\odot}$ at ~ 60 AU to $\sim 0.005 M_{\odot}$ at $\gtrsim 300$ AU. High-resolution optical spectroscopy showed no evidence for a double-line spectroscopic binary (Dahm et al. 2012).

EPIC 205151387 also has strict limits on close companions from extensive AO imaging. Companions are ruled out from $\sim 0.03 M_{\odot}$ at ~ 2 AU to $\sim 0.01 M_{\odot}$ at ~ 40 AU (Kraus et al. 2008) and from $\sim 0.10 M_{\odot}$ at ~ 60 AU to $\sim 0.008 M_{\odot}$ at $\gtrsim 300$ AU (Ireland et al. 2011). High-resolution optical spectroscopy showed no signs of a double-line spectroscopic binary (Dahm et al. 2012).

EPIC 203850058 is an ultra-cool brown dwarf, making it a particularly difficult target for AO imaging. We do not know of any existing AO data for this source.

4 DISCUSSION

4.1 Disk Inclinations

For EPIC 204638512, we adopt the disk inclination of $i = 6^{\circ} \pm 1.5^{\circ}$ derived by Mathews et al. (2012), who placed strong constraints on disk geometry using their ^{12}CO first-moment map and assumptions of Keplerian rotation. For EPIC 205151387 and EPIC 203850058, we derive disk inclinations from their sub-mm continuum data (Section 3.2) using standard routines from the *Common Astronomy Software Applications* (CASA) package (McMullin et al. 2007); although their existing CO data were insufficient to derive precise disk inclinations, the first-moment maps can be used as rough checks on our continuum results.

We derived the disk inclination of EPIC 205151387 using the CASA routine `uvmodelfit`, which fits simple analytic source component models (point-source, Gaussian, or disk) directly to the visibility data. We assumed an elliptical Gaussian model, which has six free parameters: integrated flux density (F), FWHM along the major axis (a), aspect ratio of the axes (r), position angle (PA), right ascension offset from the phase center ($\Delta\alpha$), and declination offset from the phase center ($\Delta\delta$). We found $F = 49.5 \pm 0.4$ mJy and $\text{PA} = -22^{\circ} \pm 3^{\circ}$, then derived the inclination from r assuming circular disk structure, finding $i = 53^{\circ} \pm 2^{\circ}$. To check our results, we analyzed the first-moment ^{12}CO map, finding a similar position angle ($\text{PA} \approx -30^{\circ}$) and inclination ($i \approx 50^{\circ}$) when assuming Keplerian rotation.

EPIC 203850058 is thought to have a high disk inclination based on the detection of an optical jet (Whelan et al. 2005) and the nearly symmetric morphology of a bipolar outflow in molecular CO (Phan-Bao et al. 2008), as previously noted by Ricci et al. (2012). To derive an inclination, we again used `uvmodelfit` to fit an elliptical Gaussian model to the continuum visibility data, but with an initial guess of $\text{PA} \approx 20^{\circ}$ based on the first-moment ^{12}CO map in Ricci et al. (2012). We found $F = 4.0 \pm 0.1$ mJy and $\text{PA} = 15^{\circ} \pm 1^{\circ}$, consistent with Ricci et al. 2012. We then derived the inclination from r assuming circular disk structure, finding $i \approx 90^{\circ}$, but with very large errors. We therefore checked our results with the CASA routine `imfit`, which fits an elliptical Gaussian to the source in its image plane, then uses the clean beam to return de-convolved fit results; we found a nearly edge-on disk with $i = 73^{\circ} \pm 23^{\circ}$, $F = 4.2 \pm 0.1$ mJy, and $\text{PA} = 10^{\circ} \pm 15^{\circ}$. Although the small size and faint emission of this source complicates the analysis, the overall picture appears to point to a nearly edge-on viewing geometry for EPIC 203850058.

Note that these sub-mm observations have resolutions of ~ 20 – 50 AU in radius (Section 3.2), thus the estimated inclinations reflect bulk disk geometry and assume a uniform inclination angle throughout the disk. Moreover, the uncertainties do not include systematic errors (e.g., we assume the observed disks of EPIC 205151387 and EPIC 203850058 are adequately represented by elliptical Gaussians).

4.2 A Call For Re-thinking Dipper Mechanisms

The proposed mechanisms explaining the dipper phenomenon favor geometries that are nearly edge-on. The disks are likely not seen completely edge-on ($i = 90^{\circ}$), however, due to the moderate extinction towards the dippers ($A_V \lesssim 1$; Ansdell et al. 2016). Rather, it is thought that we are viewing the dippers at nearly edge-on inclinations (e.g., $i = 70^{\circ}$) and thus observing transits of occulting material lifted above the disk midplane by some process (e.g., the breakdown of Rossby waves into vortices; Ansdell et al. 2016). Notably, none of the proposed dipper mechanisms can account for obscurations from face-on disks.

Thus the surprising range of dipper disk inclinations presented in this work, in particular the face-on geometry of EPIC 204638512 (J1604-2130), suggests that nearly edge-on viewing geometries are *not* a defining characteristic of the dippers and motivates the exploration of alternative models (or combinations of models) that can explain a range of disk inclinations. For example, occulting accretion streams (e.g., McGinnis et al. 2015; Bodman et al. 2016) could possibly account for even face-on outer disks if they act in concert with other mechanisms warping the inner disk, such as dynamical interactions with (proto-) planets or low-mass stellar companions (e.g., Facchini et al. 2014; Marino et al. 2015). Populations of scattered planetesimals from migrating (proto-) planets may also explain low dipper disk inclinations (Krijt & Dominik 2011), but more work is needed to explore nearly polar orbits.

4.3 EPIC 204638512 (J1604-2130)

EPIC 204638512 is a particularly interesting case. This source hosts a face-on disk ($i = 6^{\circ} \pm 1.5^{\circ}$; Mathews et al.

2012) with a large sub-mm dust cavity (~ 80 AU in radius; Zhang et al. 2014), which seemingly makes it an unlikely dipper. Yet, EPIC 204638512 exhibits the deepest flux dips among the known K2 dippers (up to $\sim 60\%$; Figure 1). How can these characteristics be reconciled?

The dipper activity may be related to an inclined and variable inner dust disk, as implied from its infrared emission. The object's *Spitzer* IRAC photometry shows no excess (Mathews et al. 2012), while its *Spitzer* IRS spectrum and WISE photometry reveal excesses consistent with dust at small ($\lesssim 0.1$ AU) orbital radii (Dahm 2010; Zhang et al. 2014). A factor of four variability in mid-infrared flux was also seen over several weeks, indicating a rapidly changing inner dust disk (Dahm & Carpenter 2009). Moreover, Takami et al. (2014) used near-infrared imaging polarimetry to identify intensity nulls in the outer disk annulus, which could be self-shadowing from a misaligned inner disk.

An inclined transient inner disk has been proposed for HD 142527, which also hosts a face-on transition disk with a large inner dust gap (Fukagawa et al. 2006) and exhibits intensity nulls along the outer disk annulus in its infrared scattered light images (Casassus et al. 2012). HD 142527 has a known inner disk, thought to be a transient feature of accretion from the outer disk (Verhoeff et al. 2011; Casassus et al. 2013). Marino et al. (2015) modeled the system, finding a relative inclination of $\sim 70^\circ$ between the inner and outer disks, possibly due to dynamical interactions with a low-mass stellar companion orbiting inside the dust gap (Biller et al. 2012; Rodigas et al. 2014; Close et al. 2014).

A similar scenario for EPIC 204638512 would reconcile its dips and face-on outer disk. One indication of an inclined inner disk is EPIC 204638512's weak rotational signal (Section 3.1), which suggests the star is pole-on and thus aligned with the outer disk. The dust cavity of EPIC 204638512 is also thought to have been cleared by giant planet(s) orbiting inside the dust gap (Mathews et al. 2012; Zhang et al. 2014; van der Marel et al. 2015), which could drive an inner disk warp. However, giant planets alone likely cannot account for all the dippers, as dipper occurrence rates (e.g., $\sim 20\text{--}30\%$ in NGC 2264; Alencar et al. 2010; Cody et al. 2014) are much larger than giant planet occurrence rates around late-type stars (e.g., a few percent; see Figure 8 in Gaidos et al. 2013).

5 SUMMARY

We presented disk inclinations for the three known dippers with resolved sub-mm data. We found disks with a range of viewing geometries, most notably the face-on transition disk J1604-2130. Our findings show that nearly edge-on disk inclinations are *not* a defining characteristic of the dippers, contrary to the currently proposed mechanisms explaining the dips, suggesting that additional models should be explored. Resolving more dipper disks with ALMA, and exploring techniques such as spectroastrometry that can directly probe the inner disk (e.g. Pontoppidan et al. 2008), will be essential to understanding and properly interpreting the dippers in the context of planet formation.

ACKNOWLEDGEMENTS

Support comes from NSF grant AST-1208911 (MA), NASA grants NNX11AC33G (EG) & NNX15AC92G (JPW), ERC grant 279973 (MCW), Hubble Fellowship 51364 (AWM), and a Royal Society University Research Fellowship (GK).

REFERENCES

- Alencar S. H. P., et al., 2010, *A&A*, **519**, A88
- Andrews S. M., Williams J. P., 2007, *ApJ*, **671**, 1800
- Ansdell M., et al., 2016, *ApJ*, **816**, 69
- Biller B., et al., 2012, *ApJ*, **753**, L38
- Bodman E. H. L., et al., 2016, preprint, ([arXiv:1605.03985](https://arxiv.org/abs/1605.03985))
- Bouvier J., et al., 1999, *A&A*, **349**, 619
- Carpenter J. M., Ricci L., Isella A., 2014, *ApJ*, **787**, 42
- Casassus S., Perez M. S., Jordán A., Ménard F., Cuadra J., Schreiber M. R., Hales A. S., Ercolano B., 2012, *ApJ*, **754**, L31
- Casassus S., et al., 2013, *Nature*, **493**, 191
- Close L. M., et al., 2014, *ApJ*, **781**, L30
- Cody A. M., et al., 2014, *AJ*, **147**, 82
- Dahm S. E., 2010, *AJ*, **140**, 1444
- Dahm S. E., Carpenter J. M., 2009, *AJ*, **137**, 4024
- Dahm S. E., Slesnick C. L., White R. J., 2012, *ApJ*, **745**, 56
- Facchini S., Ricci L., Lodato G., 2014, *MNRAS*, **442**, 3700
- Fukagawa M., Tamura M., Itoh Y., Kudo T., Imaeda Y., Oasa Y., Hayashi S. S., Hayashi M., 2006, *ApJ*, **636**, L153
- Gaidos E., Fischer D. A., Mann A. W., Howard A. W., 2013, *ApJ*, **771**, 18
- Ho P. T. P., Moran J. M., Lo K. Y., 2004, *ApJ*, **616**, L1
- Howard A. W., et al., 2010, *Science*, **330**, 653
- Howell S. B., et al., 2014, *PASP*, **126**, 398
- Ireland M. J., Kraus A., Martinache F., Law N., Hillenbrand L. A., 2011, *ApJ*, **726**, 113
- Kraus A. L., Ireland M. J., Martinache F., Lloyd J. P., 2008, *ApJ*, **679**, 762
- Krijt S., Dominik C., 2011, *A&A*, **531**, A80
- Manara C. F., Testi L., Natta A., Alcalá J. M., 2015, *A&A*, **579**, A66
- Marino S., Perez S., Casassus S., 2015, *ApJ*, **798**, L44
- Mathews G. S., Williams J. P., Ménard F., 2012, *ApJ*, **753**, 59
- McClure M. K., et al., 2010, *ApJS*, **188**, 75
- McGinnis P. T., et al., 2015, *A&A*, **577**, A11
- McMullin J. P., Waters B., Schiebel D., Young W., Golap K., 2007, in Shaw R. A., Hill F., Bell D. J., eds, *Astronomical Society of the Pacific Conference Series Vol. 376, Astronomical Data Analysis Software and Systems XVI*. p. 127
- Morales-Calderón M., et al., 2011, *ApJ*, **733**, 50
- Natta A., Testi L., Comerón F., Oliva E., D'Antona F., Baffa C., Comoretto G., Gennari S., 2002, *A&A*, **393**, 597
- Natta A., Testi L., Muzerolle J., Randich S., Comerón F., Persi P., 2004, *A&A*, **424**, 603
- Pecaut M. J., Mamajek E. E., Bubar E. J., 2012, *ApJ*, **746**, 154
- Petigura E. A., Marcy G. W., Howard A. W., 2013, *ApJ*, **770**, 69
- Phan-Bao N., et al., 2008, *ApJ*, **689**, L141
- Pontoppidan K. M., Blake G. A., van Dishoeck E. F., Smette A., Ireland M. J., Brown J., 2008, *ApJ*, **684**, 1323
- Ricci L., Testi L., Natta A., Scholz A., de Gregorio-Monsalvo I., 2012, *ApJ*, **761**, L20
- Rodigas T. J., Follette K. B., Weinberger A., Close L., Hines D. C., 2014, *ApJ*, **791**, L37
- Silburt A., Gaidos E., Wu Y., 2015, *ApJ*, **799**, 180
- Skrutskie M. F., et al., 2006, *AJ*, **131**, 1163
- Takami M., et al., 2014, *ApJ*, **795**, 71
- Vanderburg A., Johnson J. A., 2014, *PASP*, **126**, 948
- Verhoeff A. P., et al., 2011, *A&A*, **528**, A91

Whelan E. T., Ray T. P., Bacciotti F., Natta A., Testi L., Randich S., 2005, [Nature](#), **435**, 652
Zhang K., Isella A., Carpenter J. M., Blake G. A., 2014, [ApJ](#), **791**, 42
van der Marel N., van Dishoeck E. F., Bruderer S., Pérez L., Isella A., 2015, [A&A](#), **579**, A106

This paper has been typeset from a $\text{\TeX}/\text{\LaTeX}$ file prepared by the author.